Pore Formation in Lipid Bilayer Membranes Made of Phosphatidylinositol and Oxidized Cholesterol Followed by Means of Alternating Current

Enrico Gallucci,* Silvia Micelli,* and Gianluigi Monticelli#
*Dipartimento Farmaco-Biologico, Università degli Studi, 70126 Bari, and #Istituto di Fisiologia e Chimica Biologica, Università degli Studi, 20144 Milano, Italy

ABSTRACT The kinetics of porin incorporation into black lipid membranes (BLM) made of phosphatidylinositol (PI) or oxidized cholesterol (Ox Ch) were studied by means of alternating current; the set-up was able to acquire resistance and capacitance simultaneously by means of a mixed double-frequency approach at 1 Hz and 1 KHz, respectively. Conductance was dependent on the interaction between protein-forming pores and lipids. For PI membranes below a porin concentration of 12.54 ng/ml, there was no membrane conductivity, whereas at 200 ng/ml a steady-state value was reached. Different behavior was displayed by Ox Ch membranes, in which a concentration of 12.54 ng/ml was sufficient to reach a steady state. The incorporation kinetics when porin was added after membrane formation were sigmoidal. When porin was present in the medium before membrane formation, the kinetics were sigmoidal for PI membranes but became exponential for Ox Ch membranes. Furthermore, for BLM made of PI, the conductance-versus-porin concentration relationship is sigmoidal, with a Hill coefficient of 5.6 ± 0.07, which is functional evidence corroborating the six-channel repeating units seen previously. For BLM made of Ox Ch, this relationship followed a binding isotherm curve with a Hill coefficient of 0.934 ± 0.129.

INTRODUCTION

The complexity of biological membranes and the experimental difficulties associated with the investigation of their functions and properties in intact cells led to an attempt to make membrane models.

Mueller et al. (1962) reported the reconstitution of planar lipid membranes with properties fairly similar to those of biological membranes.

Structures made "in vitro" have several advantages: their composition is easy to manipulate, substances can be incorporated, and electrical measurement is simple. Moreover, the incorporation of proteins into the bilayer allows for investigations of the interrelationships between membrane components. In particular, investigating the macroscopic incorporation of channels may be of relevance to understanding the physiological mechanism underlying channel assembly in cell membranes as a function of different parameters. In fact, it is known that some physiological signals govern the change in cellular ionic composition (Els and Chou, 1993), by means of modulation or recruitment of the channels.

Electrophysiological equipment offers the best tool for studying the kinetics of incorporation of these channels into BLM. Previous works have involved the use of direct current (DC).

The electrical parameters of the membrane can also be measured by means of alternating current (AC), which offers the advantage of eliminating the effect of possible electrode polarization (Ti Tien and Diana, 1968).

Received for publication 2 October 1995 and in final form 23 April 1996.
Address reprint requests to Dr. Enrico Gallucci, Dipartimento Farmaco-Biologico, Università degli Studi, V. E. Orabona 4, 70126 Bari, Italy. Tel.: 39-80-5442796; Fax: 39-80-5442770; E-mail: gallucci@farmbiol.uniba.it.

0006-3495/96/08/824/08 $2.00

Until now AC has been exclusively utilized for capacitance measurements, but to our knowledge this is the first time that AC has been used to monitor the capacitance and the resistance of the membrane continuously and simultaneously. This method has the advantage of continuously monitoring resistance and capacitance as a function of time during pore formation until a steady state of the phenomenon is reached.

The aim of this research was to optimize an experimental set-up using alternating current to study the electrical properties of BLM during pore or channel incorporation in kinetic condition and at the steady state of the phenomenon.

Preliminary reports of this paper were presented at the Tenth School on the Biophysics of Membrane Transport, Szczyrk, Poland (Monticelli et al., 1990).

MATERIALS AND METHODS

Materials

PI was extracted from ox brain following the method of Folch (1942), and the purity was chromatographically checked using thin-layer chromatography, with chloroform/methanol/acetic acid/water (100/50/16/2) as the solvent system. Ox Ch was obtained following the method of Ti Tien et al. (1966). Porin purified from bovine heart mitochondria (De Pinto et al., 1987) was kindly furnished by Prof. Ferdinando Palmieri (Dipartimento Farmaco-Biologico, University of Bari, Bari, Italy). The protein was added to aqueous phases from a concentrated stock solution containing 0.1% Triton X-100. The final aqueous Triton X-100 concentration in the experimental chamber was 0.00012% at the highest porin concentration used. *n*-Decane and octane were from Fluka (Puriss, Buchs, Switzerland). KCl, chloroform, methanol, and acetic acid (RPE) were from Carlo Erba (Milan, Italy). The thin-layer chromatography plates were from Merck (Kielsegel 60, Darmstadt, Germany). Water was double distilled in a commercial apparatus.

The cell

Experiments were performed in a classical Teflon chamber similar to that described by Läuger et al. (1967). The volume of each compartment was 4

ml, and the circular aperture between the two compartments had a diameter of 1.3 mm.

The compartments were filled with KCl solutions of varying concentrations and mechanically stirred. The aqueous salt solutions were buffered at pH 7.0.

Membranes were formed from a solution of 1% (w:v) of PI in *n*-decane or Ox Ch in octane-*n*-decane by brushing the lipid solution across the aperture of the cell (Mueller et al., 1962, 1969).

Experiments were performed at a room temperature of 22–24 ± 1°C.

The electrical device

The circuit theory appropriate to a system considering the membrane and the aqueous phases as well as stray capacitance has been described by Hanai et al. (1969) and Ohki (1969).

Electrically, the membrane was considered as a parallel combination of a resistance and a capacitance. To measure these two quantities simultaneously, two mixed frequencies, 1 Hz (variable Vpp) and 1 kHz (2 mVpp), were used (Fig. 1).

The complete system lumped circuit, with the membrane electrical equivalent included, is represented in Fig. 2, where R_m and C_m are the membrane resistance and the capacitance, and R_l and C_l are those of the current-to-voltage converter or measurement device, which may vary according to experimental conditions, but usually R_l = 1 MΩ and C_l = 10–100 nF were used. R_a and C_a represent the ionic solution, and C_b is the stray capacitance.

The signal V_s was applied as input voltage to a Pt electrode on one cell side; the output signal, V_l, was acquired through a second Pt electrode placed on the other side of the cell.

V_l was then used as input to the measuring instrument, which consisted of a variable impedance input circuit and a passband amplifier, followed by a frequency splitter able to separate the 1-Hz cell output signal from the 1-kHz component (Fig. 1).

Once split, the 1-Hz component (V_l) and the 1-kHz component were recorded with a strip chart recorder (LKB 102; Pharmacia LKB Biotechnology AB, Uppsala, Sweden) or processed by means of a computer (on line). The 1-kHz component was used to calculate C_m by means of a calibration curve obtained with a series of known capacitances. V_l and C_m are then used to compute the membrane resistance R_m by means of a three-equation system (see below).

Analysis of electrical parameters for the measurements without the membrane

If we consider the electrical equivalent circuit reported in Fig. 2, without the component R_mC_m relative to the membrane, the stray capacitance for the whole system was less than 150 pF.

With bathing solutions the experimental chamber was checked to evaluate resistance and phase angle values. In these conditions the total current crossing the circuit is

$$\bar{I} = \bar{I}_{Ra} + \bar{I}_{Ca} + \bar{I}_{Cb} = \bar{I}_{Rl} + \bar{I}_{Cl}. \qquad (1)$$

As V_s is the imposed voltage, V_l is measured, and R_l and C_l are known, φ_l (the angle phase of V_l) is determined ($\tan\varphi_l = \omega R_l C_l$, where $\omega = 2\pi\nu$).

Without the measurements of R_a, C_a, and C_b, the limiting values of φ_s (the phase angle of V_s) can be calculated by referring to the vector scheme in Fig. 3, considering that $-\pi/2 < \varphi_a < 0$ (*RC* circuit).

The applied voltage is $\bar{V}_s = \bar{V}_l + \bar{V}_a$, and therefore the two limit positions (ϑ_1 and ϑ_2) of $\bar{V}_s$ (Fig. 3) can be calculated, considering that $V_s \cos\vartheta_2 = V_l \cos\varphi_l$, $V_s \sin\vartheta_1 = V_l \sin\varphi_l$, so that $\vartheta_2 < \varphi_s < \vartheta_1$.

In Table 1, as an example, the ϑ_1 and ϑ_2 values, as well as $\varphi_l - \vartheta_1$ and $\varphi_l - \vartheta_2$, in KCl solutions (0.5 and 1 M) are reported. Under these conditions, following the vector scheme in Fig. 3, $\bar{V}_l$ and $\bar{V}_s$ proved to be in phase.

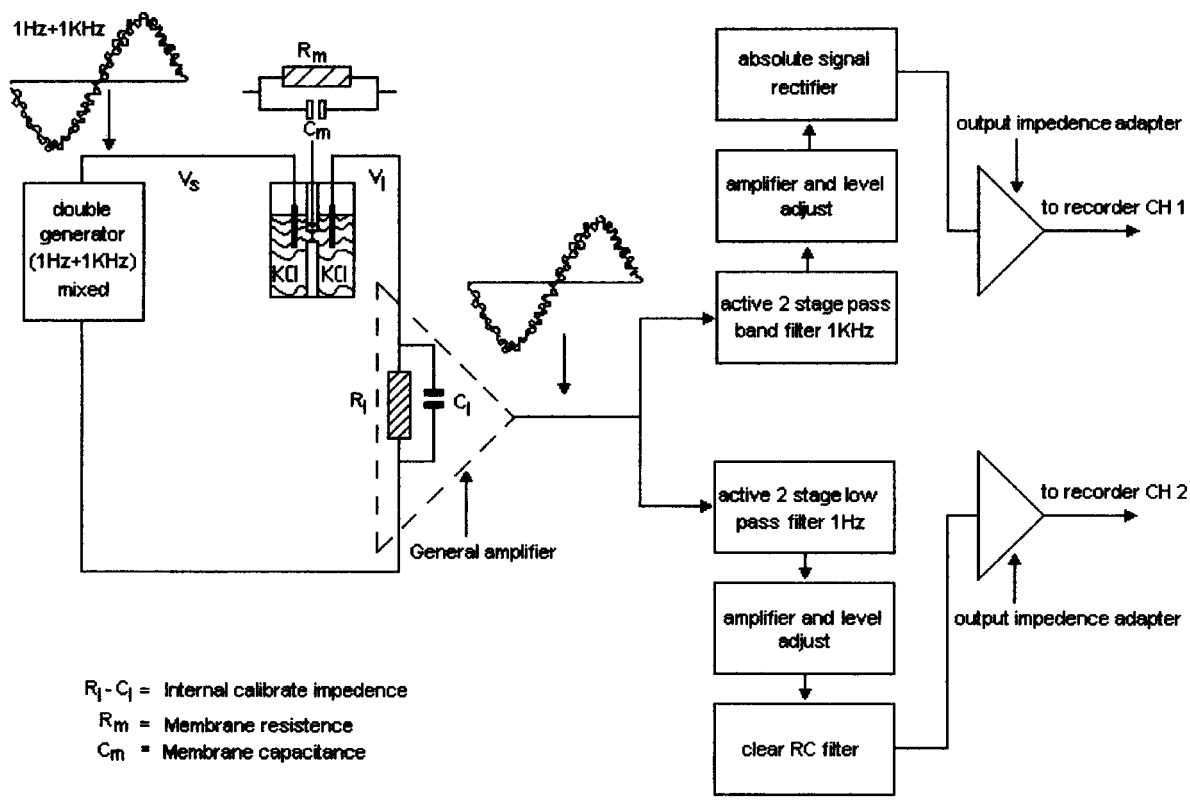

FIGURE 1 Block diagram of the electrical circuit.

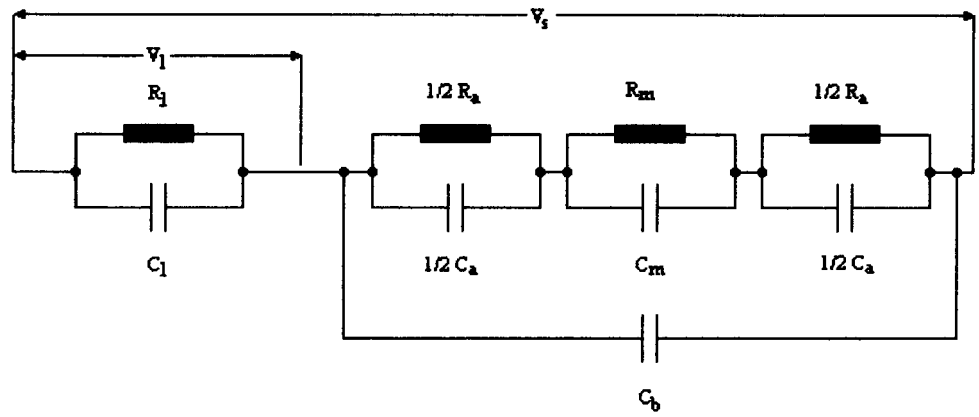

FIGURE 2 Complete equivalent circuit of the experimental apparatus when the membrane is formed in the hole of the wall separating the two compartments of the chamber. In this scheme membrane (m), ionic solutions (a), stray capacitance (b), and the measurement device (l) are represented.

At different KCl concentrations and for a given applied voltage, the V_l values measured did not differ significantly, giving R_a in the range 10–20 KΩ. No significantly different value of R_a could be calculated for $C_a + C_b$, which varied below 200 pF (data not reported).

In all of the test conditions, the resistance values of the experimental chamber with ionic solutions were very low compared to those of the membranes (on the order of MΩ). The phase angle value was close to that of the measuring device ($\varphi_l = 0.561$ rad or 0.063 rad, with $R_l = 1$ MΩ and $C_l = 100$ or 10 nF, respectively).

An auxiliary simulation was run by putting porin, at different concentrations, in the bathing solution without the membrane. Variable voltage, V_s, was then applied; in none of these experiments could any differences between output voltage, V_l and V_s, be recorded. These experiments are designed to exclude any artifact due to porin "per se."

Analysis of electrical parameters for the measurements with the membrane

For the conditions described above, neglecting the resistance and the capacitance of the ionic solutions and the stray capacitance, the membrane equivalent circuit, R_mC_m, was considered simply in series with an analogous circuit of the measuring device, and input voltage ($V_s(t) = V_s \sin \omega t$) was applied to the whole series as shown in the simplified circuit in Fig. 4.

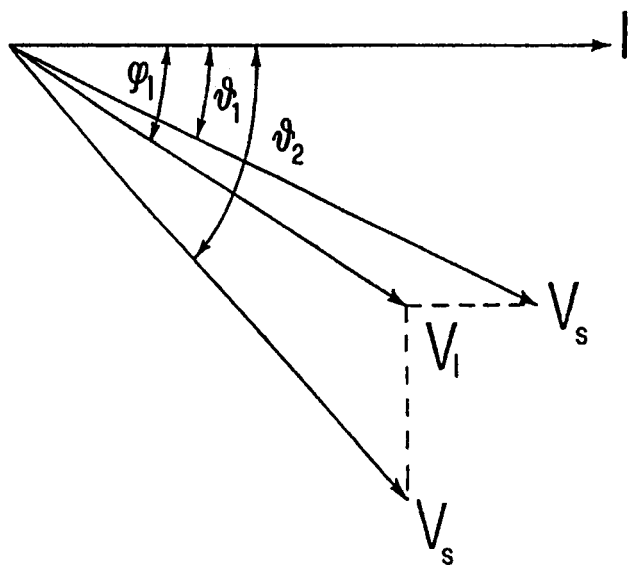

FIGURE 3 Estimation of V_s limit positions without the membrane formed.

In this circuit the applied voltage is $\bar{V}_S(t) = \bar{V}_M(t) + \bar{V}_L(t)$, where $V_M(t) = V_m(t)\sin(\omega t - \beta)$ and $V_L(t) = V_l(t)\sin(\omega t + \alpha)$ (Fig. 5).

The current crossing the resistance and capacitance of the measuring device is $I_{rl} = G_lV_l = V_l/R_l$ and $I_{cl} = B_lV_l = \omega C_lV_l$, where $G_l = 1/R_l$ and $B_l = 1/X_l = \omega C_l$ and the total current is

$$I = (I_r^2 + I_c^2)^{1/2}. \tag{2}$$

With the vector graph reported in Fig. 5 the following relationships are obtained:

$$V_l \cos(\varphi - \varphi_l) + V_m \cos(\varphi_m - \varphi) = V_s \tag{3}$$

$$V_l \sin(\varphi - \varphi_l) = V_m \sin(\varphi_m - \varphi), \tag{4}$$

and when C_m has been measured, a third equation,

$$\omega C_m V_m = I \sin \varphi_m, \tag{5}$$

can be written.

As V_s is imposed, ω and φ_l are constant, V_l and C_m are measured, and I is calculated by means of Eq. 2, this system of equations (Eqs. 3–5) can be utilized to determine the phase angle φ, φ_m, and the voltage V_m.

The membrane conductance G_m ($= 1/R_m$) can be calculated by the current crossing the resistive part of the membrane:

$$I_{rm} = G_mV_m = I \cos \varphi_m.$$

From the analysis mentioned above, it is sufficient to measure V_l and C_m to determine the membrane current and conductance, and from that, information on the kinetics of channel formation during porin incorporation can be obtained.

Because of the electrical circuit adopted, the measurement of V_l is strictly related to the electrical current crossing the membrane. A close, classical relationship is valid at $t = 0$ (before adding porin molecules to the bathing solutions) and at the steady state of porin incorporation.

TABLE 1 Limit positions of the phase angles between V_m and V_l, in the absence of a lipid membrane, following the vector scheme in Fig. 3

KCl (M)	n	ϑ_l (rad)	ϑ_2 (rad)	$\varphi_l - \vartheta_l$ (rad)	$\varphi_l - \vartheta_2$ (rad)
1.0	67	0.544 ± 0.002	0.589 ± 0.004	0.013 ± 0.002	−0.032 ± 0.004
0.5	17	0.552 ± 0.000	0.584 ± 0.001	0.009 ± 0.000	−0.023 ± 0.001

$R_l = 1$ MΩ; $C_l = 100$ nF.

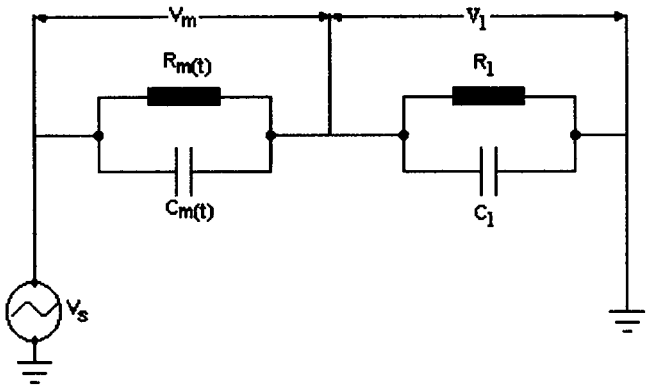

FIGURE 4 Equivalent circuit of the membrane (m) and of the measurement device (l). The source voltage V_s is applied to the whole series. V_m and V_l are the membrane and output voltages, respectively. R_l is the electrical resistance and C_l the capacitance of the measuring circuit; $R_m(t)$ and $C_m(t)$ are the membrane electrical resistance and capacitance, respectively. During pore formation the membrane electrical resistance and capacitance are time dependent.

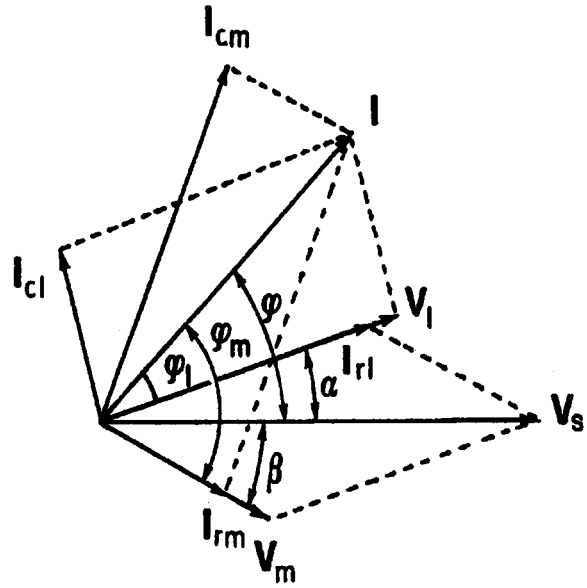

FIGURE 5 Vector scheme of voltages and currents in the circuit of Fig. 4

Performance of the apparatus

The whole set-up was checked with an equivalent circuit, simulating the porin-induced and the porin-free membrane conductances. It consisted of a series of combinations of a resistance and a capacitance in parallel of appropriate magnitude. The R_m and C_m values calculated from the output signal correspond to the resistance and capacitance tests.

Data analysis

The equations were solved by a computer program, Eureka; the data were analyzed by fitting a curve using nonlinear regression by means of a computer program, GraphPad. In brief, nonlinear regression procedures, through an iterative process, are used to determine values of the parameters that minimize the sum of the squares of the distances between the data points and the curve.

Results are expressed as mean ± SE. Statistical significance was determined by Student's *t*-test, performed by means of the Instat program (GraphPad). In the figures the number of experiments is given near each point.

RESULTS

Electrical parameters of the BLM versus KCl concentrations

For KCl concentrations of 0.1, 0.5, and 1 M, the capacitances and the specific conductances, G_m, are reported in Tables 2 and 3, respectively.

Conductance and capacitance were higher in Ox Ch membranes as compared to PI membranes. These results are in accordance with those of other authors obtained with direct current methods (Lesslauer et al., 1967; Ti Tien and Diana, 1968; Rosen and Sutton, 1968).

Electrical parameters of BLM with porin added after or before membrane formation

To gather information on the kinetic conditions, porin was added to both compartments after the membrane had turned optically black or before membrane formation.

As it was found that porin conductance was higher at 1 M KCl concentration (Benz, 1986a,b; Colombini, 1986), the porin incorporation experiments were performed at this ionic concentration. The addition of porin to the solutions bathing a black membrane resulted in an increase in output voltage V_l. This increase was time dependent, indicating protein insertion and pore formation inside the lipid matrix. A steady-state value of V_l was found to depend on porin concentration, as discussed below. After the membrane broke, V_l returned to the imposed voltage V_s (Fig. 6).

In PI and Ox Ch membranes, different kinetics were obtained in experimental conditions where the porin molecules were added in aqueous solutions before membrane formation. In fact, in PI membranes the time course of the V_l was sigmoidal (Fig. 7 *A*), irrespective of porin addition before or after membrane formation. When porin was added before membrane formation, however, a delay in channel formation and a slower kinetics were observed.

All of the S-shaped curves were fitted by means of a four-parameter logistic equation:

$$V_l(t) = A + B/\{1 + 10^{D(C-t)}\}, \quad (6)$$

where $A = V_l(0)$ is the V_l at $t = 0$ (at membrane black), $B = V_{lss} - V_l(0)$ is the steady-state value of the voltage V_l at the end of the protein incorporation and channel formation

TABLE 2 Conductance (G_m) and capacitance (C_m) of PI membranes at different KCl concentrations

KCl (M)	*n*	G_m (μS/cm^2)	C_m (nF/cm^2)
0.1	85	2.68 ± 0.12*	299.00 ± 7.79**
0.5	93	2.92 ± 0.12**	271.77 ± 5.55***
1.0	225	2.38 ± 0.06	249.00 ± 4.60

Significant changes $p = 0.0147$ (*), $p = 0.0001$ (**), and $p = 0.0047$ (***), assessed on a paired basis relative to 1 M KCl values, are indicated.

TABLE 3 Conductance (G_m) and capacitance (C_m) of Ox Ch membranes at different KCl concentrations

KCl (M)	n	G^m (μS/cm^2)	C_m (nF/cm^2)
0.1	67	4.85 ± 0.12	451.72 ± 11.43**
0.5	33	4.27 ± 0.20	468.40 ± 38.90*
1.0	113	5.11 ± 0.24	404.47 ± 9.09

Significant changes $p = 0.0183$ (*) and $p = 0.0016$ (**), assessed on a paired basis relative to 1 M KCl values, are indicated.

process, C is the time to half-maximum value, and D is the Hill coefficient or slope factor.

In Ox Ch membranes, the time course of the voltage V_1 was sigmoidal when the porin was added after membrane formation. It was exponential, however, when the porin was present before membrane formation (Fig. 7 *B*) in particular: no time lag was observed, V_1 started at a higher value, and the kinetics were faster.

These exponential curves in Ox Ch membranes were fitted by

$$V_1(t) = A^*(1 - e^{-t/\tau}) + C, \quad (7)$$

where $A = V_{lss} - V_1(0)$, τ is the time constant of the kinetics, and $C = V_1(0)$ is the value of V_1 at $t = 0$.

According to Eqs. 6 and 7, fitting procedures make it possible to determine the characteristic parameters $V_1(0)$, V_{lss}, and the derivative value of $V_1 = f(t)$, i.e., the maximum rate of channel incorporation or maximum depolarization rate $[dV_1/dt_{max}]$.

Besides, the time lag between porin addition and the first current variation was shorter in Ox Ch than in PI membranes; in fact, for the same porin concentration (asterisks and open circles in Figs. 8, *B* and *A*, respectively), the incorporation kinetics were faster, with higher steady-state levels being reached.

In both types of membranes, porin incorporation kinetics depended on protein concentration (protein added after membrane formation): four kinetics of porin incorporation in PI membranes and five kinetics in Ox Ch membranes are plotted in Fig. 8, *A* and *B*, respectively .

At constant applied voltage V_s, the steady-state value of V_1, V_{lss}, increased with porin concentration in bathing solutions. In the case of PI membranes (Fig. 9 *A*), this dependence was studied as a function of porin concentration up to 200 ng/ml. It can be seen that V_{lss} increased slowly until the porin concentration had reached 35–40 ng/ml; the slope then steepened and flattened to form an S-shaped function.

In Ox Ch membranes, the relation V_{lss} versus C_{por} shows hyperbolic behavior, the slope being almost parallel to the y axis. As shown in Fig. 10 *A*, the maximum V_{lss} value was reached with a porin concentration of about 8 ng/ml.

With respect to the maximum depolarization rate, $[dV_1/dt]_{max}$, PI membranes exhibited curves similar to those of V_{lss} as a function of C_{por}. A slow increase in the incorporation rate (Fig. 9 *B*) was obtained at a porin concentration of up to 35 ng/ml; at higher values of C_{por} the slope was much steeper,

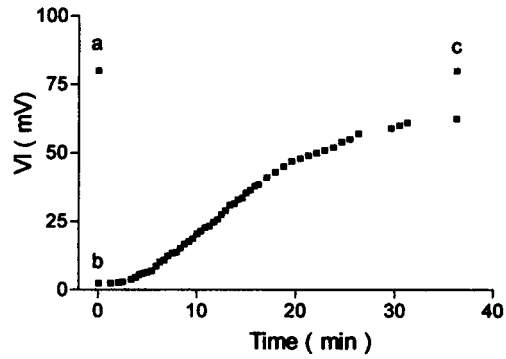

FIGURE 6 Output voltage (V_1) as a function of time in a representative experiment in which porin (62.7 ng/ml) was added at $t = 0$ to both sides of the black PI membrane. $V_s = 40$ mV. V_1 value with bathing solution but without the membrane (*a*), with the membrane (*b*), and after membrane breakage (*c*).

followed by saturation when the porin concentration increased further.

Completely different $[dV_1/dt]_{max}$ behavior was obtained with Ox Ch membranes (Fig. 10 *B*).

The values of V_{lss} and of the steady-state capacitance (C_{mss}) enable us to calculate the conductance at the steady state of porin incorporation ($G_{mss} - G_m(0)$). When $G_{mss} - G_m(0)$ is plotted against porin concentration (Fig. 9 *C*) in PI membranes, the porin concentration should reach a critical value (20 ng/ml) before a drastic increase in conductance is observed. A plateau is then reached at a higher protein concentration (<90 ng/ml). This curve was fitted with Eq. 6, where $A = G_m(0)$, $B = G_{mss} - G_m(0)$, and C and D have the same meaning.

With Ox Ch membranes (Fig. 10 *C*) the maximum increment in conductance is reached at low porin concentrations (6–10 ng/ml), after which a further increase in protein concentration leads to a smaller increase in G_{mss}. This curve was fitted by means of a rectangular hyperbolic equation:

$$(G_{mss} - G_m(0)) = [\text{porin}]^n G_{max}/(K_m)^n + [\text{porin}]^n, \quad (8)$$

where G_{max} is the plateau value of conductance, K_m is the dissociation constant, and n is the order of the reaction.

DISCUSSION

Despite studies devoted to biological membrane structure, there is still relatively poor understanding of lipid-protein interactions. Such studies are vital if we are to clarify such topics as the physiological relevance of the interaction of ligands and receptors, DNA transcriptions, enzymatic reactions, and pumping of ions and protons (Sekimuzu, 1994; Sachmann, 1984; Kinnunen, 1991; Bevan et al., 1989). Information from studies conducted with different methods may therefore be of help in elucidating these important topics.

The main objective of this work was to optimize a method of following the kinetics of protein incorporation

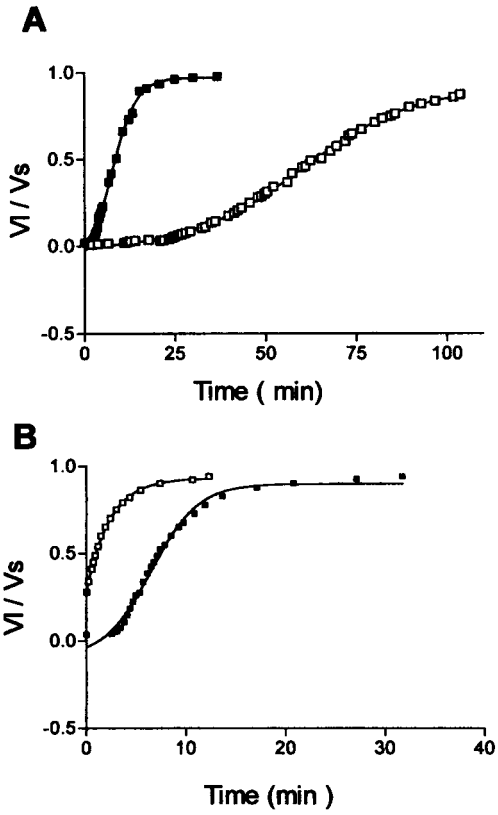

FIGURE 7 Representative experiment showing the voltage time courses at the measurement device (as the ratio of the output voltage, V_l, and the source voltage, V_s) after the addition of porin to both bathing solutions separated by black (■) and when porin is put in solution before membrane formation (□). (*A*) PI membranes: V_s = 40 mV, porin concentration 48.1 ng/ml. Parameters of sigmoidal fitting: (■) $A = -0.1419 \pm 0.039$; $B = 0.97 \pm 0.011$; $C = 7.47 \pm 0.3$; $D = 0.13 \pm 0.0081$; $r^2 = 0.997$; □, $A = -0.025 \pm 0.005$; $B = 0.91 \pm 0.009$; $C = 60.17 \pm 0.36$; $D = 0.028 \pm 0.0006$; $r^2 = 0.999$. (*B*) Ox Ch membranes: V_s = 40 mV, porin concentration 6.27 ng/ml. Parameters of sigmoidal and exponential fitting respectively: ■, $A = -0.09 \pm 0.04$; $B = 0.896 \pm 0.014$; $C = 6.5 \pm 0.24$; $D = 0.18 \pm 0.014$; $r^2 = 0.991$; □, $A = 0.65 \pm 0.005$; $B = 0.425 \pm 0.009$; $C = 0$; $D = 0$; $E = 0.28 \pm 0.004$; $t_{1/2}$ for $B = 1.63$; $r^2 = 0.999$.

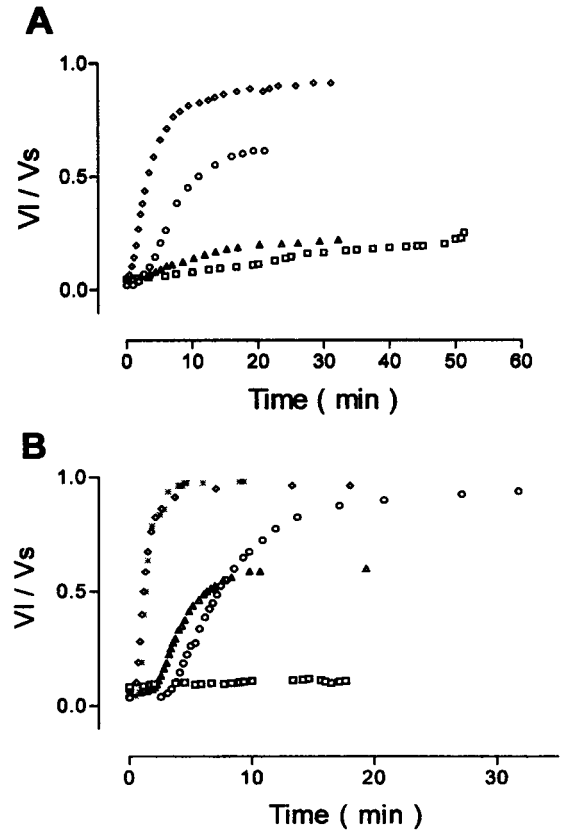

FIGURE 8 Representative experiment showing the voltage time courses at the measurement device (as the ratio of the output voltage, V_l, and the source voltage, V_s) on porin concentration (protein added after membrane was black). In all experiments V_s was 40 mV. (*A*) PI membranes. Porin concentration: □, 12.54; △, 37.6; ○, 62.7; ◇, 94.05 ng/ml. (*B*) Ox Ch membranes. Porin concentration: □, 0.13; △, 1.25; ○, 6.27; ◇, 12.54; *, 62.7 ng/ml.

into BLM, by monitoring the electrical parameters, namely conductance and capacitance. The continuous monitoring of capacitance may prove useful in tracking membrane parameters, such as thickness and dielectrical constant, that depend on the lipids and incorporated proteins.

Kinetic conditions were created by incorporating mitochondrial porin, a protein constituting the active substrates of the molecular sieves for hydrophilic substances (Rosenbusch, 1974) in the outer membrane of enteric bacteria (Nikaido and Vaara, 1985; Hancock, 1987) and mitochondria (Ludwig et al., 1986; Forte et al., 1987).

Although the use of brain lipids to make BLM is significant from a biological viewpoint, other materials, like Ox Ch, are also useful for studying induced ion conductance across membranes. In this work, two lipids of different structures were selected in the investigation of lipid-protein interaction, specifically to stress any assembly differences of a transmembrane channel into BLM.

Our experimental results and those of other authors seem to indicate that the nature of the protein-lipid interactions originates from the intrinsic properties of lipids, which, rather than simply being a support for the anchorage of the proteins, play an active role in determining protein assembly in the membrane, as the porin incorporation kinetics seems to indicate.

Qualitative similarities (S-shaped) between the kinetics curves were obtained, indicating a cooperative process of incorporation into the BLM. Considering the high activation energy required for the random incorporation, it is more likely that a protein will be incorporated into the membrane with the help of previously incorporated protein molecules. This conclusion agrees with the observation made by Zizi et al. (1995).

In Ox Ch membranes, S-shaped time behavior in channel formation was also observed, but with different kinetics parameters, i.e., the velocity of incorporation is higher, although the amount of protein in the medium is lower. These findings corroborate the observation already made by Benz et al. (1986a,b) and can be explained by considering that porin has a high affinity for sterols (Pfaller et al., 1985).

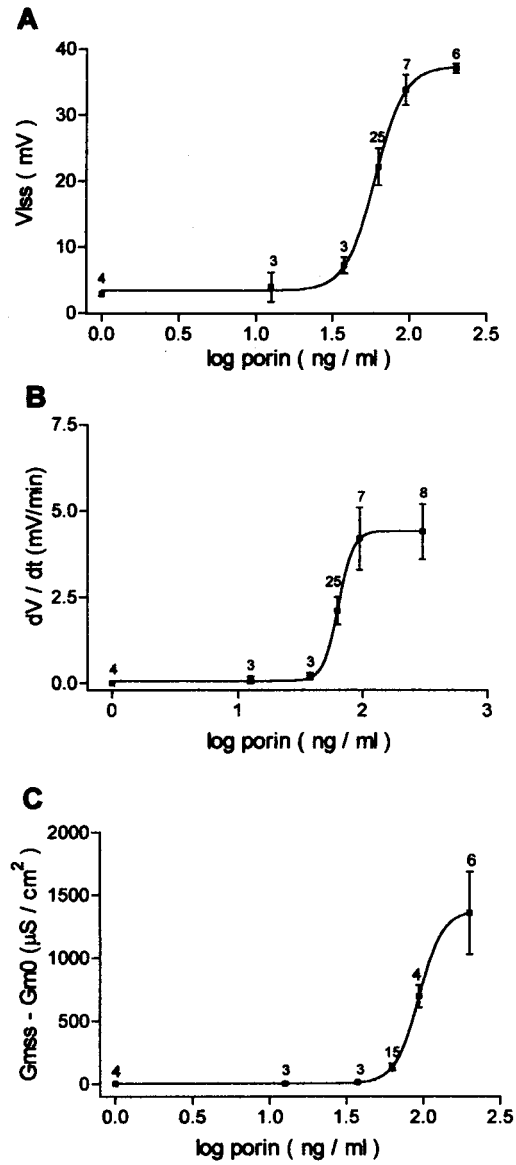

FIGURE 9 (*A*) Steady values of V_l, V_{lss}. (*B*) Maximum depolarization rate or maximum channel incorporation rate, $(dV_l/dt)_{max}$. (*C*) Specific conductance at the steady state due to channel formation ($G_{mss} - G_m(0)$) as a function of porin concentration in bathing solutions, in PI membranes. V_s = 40 mV. Fitting parameters for *C*: A = 5.37 ± 1.63; B = 1379.8 ± 3.086: C = 1.97 ± 7.5 * 10^{-4}; D = 5.6 ± 0.07; K_m = 93.83; r^2 = 1.00

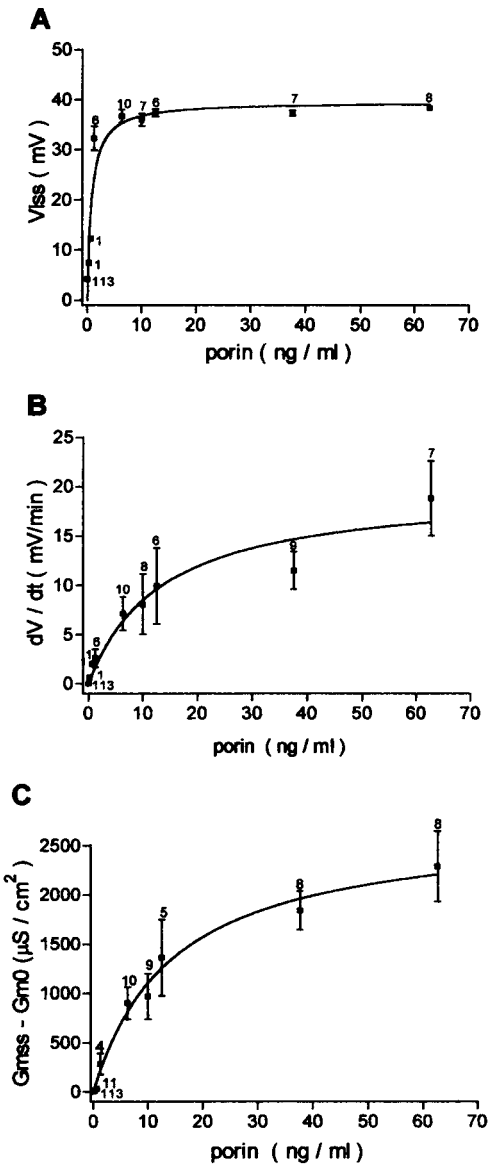

FIGURE 10 (*A*) Steady values of V_l, V_{lss}. (*B*) Maximum depolarization rate or maximum channel incorporation rate, $(dV_l/dt)_{max}$. (*C*) Specific conductance at the steady state due to channel formation ($G_{mss} - G_m(0)$) as a function of porin concentration in bathing solutions in Ox Ch membranes. V_s = 40 mV. Fitting parameters for *C*: G_{max} = 2720.39 ± 168.38; K_m = 14.59 ± 2.39; n = 0.934 ± 0.129; r^2 = 0.988.

In PI membranes, thinning to bilayer thickness took longer than in Ox Ch, as also reported by Ti Tien and Diana (1968).

When the PI membranes were drawn with porin already present in the bathing solution, the blackening time increased, indicating difficulty in the organization of the bilayer, and under these conditions pore formation was retarded, although the same steady-state kinetics value was obtained as when porin was added to the bathing solutions after membrane formation.

A speculative explanation of this finding may be that lipids with proteins improperly oriented from the torus can be drawn with this maneuver. Under these conditions, the structural changes of lipids around the protein become difficult, and consequently a longer blackening time and a delay in the further incorporation of porin are found. In other words, the interaction between phospholipid acyl chains and the hydrophobic part of the protein became stronger, thus reducing the likelihood of the first "target" driving other proteins into the bilayer.

Different behavior was shown in Ox Ch membranes, where the conductance started with a higher value and faster kinetics were obtained. This finding could suggest that porin is already organized as a channel and that porin is more likely to float in this lipid matrix.

Finally, the steady-state conductance is plotted against porin concentrations and analyzed by means of a mathematical model. A weighted least-squares fit provides an estimate of the parameters and their standard errors. In the legends to Figs. 9 *C* and 10 *C*, we report the parameters relative to a sigmoidal curve for PI membranes and a rectangular hyperbola for Ox Ch membranes, respectively.

The results indicate that K_m values are 93.83 ng/ml for PI and 14.59 ng/ml for Ox Ch membranes, which further confirms the greater affinity of porin for Ox Ch membranes.

Conductance curves for PI and Ox Ch are similar to the dependence of O_2 binding to hemoglobin and myoglobin, respectively. The cooperative behavior in PI membranes enables the Hill equation to be applied, in which the Hill coefficient (or the slope representing the order of the reaction) can be calculated. This number reflects the degree of cooperativity, in other words, the number of units of channels that are assembled in the membrane.

Although it could conceivably be due to the multimeric state of the protein in the micelle before insertion, this is rather unlikely, when we consider that the concentration of Triton X-100 is far below the critical micellar concentration (Zizi et al., 1995).

In the case of PI membranes, the Hill coefficient gives a value of 5.6 ± 0.07, and if it is permissible to compare our finding with that reported by Mannella et al. (1992) on electron microscopic images of crystalline VDAC, this value is reminiscent of the six-channel repeating units.

In the case of Ox Ch membranes, the kinetics obey a power law in which the power is 0.934 ± 0.129, indicating that a single VDAC protein constitutes the channel, according to Peng et al. (1992) and Zizi et al. (1995).

We wish to thank Mr. Nicola Ceci, Dipartimento di Fisica Università degli Studi di Bari, for building the electronics set-up. We wish to thank Prof. Claudio Lippe for his critical reading of the manuscript. We wish to thank Prof. Vittorio Picciarelli for his suggestion on the organization of the manuscript. We wish to thank the referees of this paper for their instructive suggestions. We wish to thank Anthony Green (green@pangeanet.it) for sorting out our English.

This work is dedicated to the memory of our colleague, Prof. Peter Läuger.

This work was supported in part by MPI 60% (GM), MPI 40% (EG), and CNR (92.02202.Cr14; 91.2524) grants.

REFERENCES

Benz, R. 1986a. Porin from bacterial and mitochondrial outer membranes. *CRC Crit. Rev. Biochem.* 19:145–185

Benz, R. 1986b. Analysis and chemical modification of bacterial porins. *In* Ion Channel Reconstitution. C. Miller, editor. Plenum Press, New York and London. 553–573.

Bevan, J. A., R. D. Bevan, and S. M. Shreeve. 1989. Variable receptor affinity hypothesis. *FASEB J.* 3:1696–1704.

Colombini, M. 1986. Voltage gating in VDAC. *In* Ion Channel Reconstitution. C. Miller editor. Plenum Press, New York and London. 533–552.

De Pinto, V., G. Prezioso, and F. Palmieri. 1987. A simple and rapid method for the purification of the mitochondrial porin from mammalian tissues. *Biochim. Biophys. Acta.* 905:499–502.

Els, W. J., and K. Y. Chou. 1993. Sodium-dependent regulation of epithelial sodium channel densities in frog skin: a role for the cytoskeleton. *J. Physiol. (Lond.).* 462:447–464.

Folck, J. 1942. Brain cephalin, a mixture of phosphatides. Separation from it of phosphatidylserine, phosphatidylethanolamine, and a fraction containing an inositol phosphatide. *J. Biol. Chem.* 146:35–44.

Forte, M., H. R. Guy, and C. A. Mannella. 1987. Molecular genetics of the VDAC ion channel: structural model and sequence analysis. *J. Bioenerg. Biomembr.* 19:341–350.

Hanai, T., D. A. Haydon, and J. L. Taylor. 1969. An investigation by electrical methods of lecithin in hydrocarbon films in aqueous solutions. *Proc. R. Soc. Lond.* A281:377–391.

Hancock, R. E. W. 1987. Role of porins in outer membrane permeability. *J. Bacteriol.* 169:929–933.

Kinnunen, P. K. J. 1991. On the principles of functional ordering in biological membranes. *Chem. Phys. Lipids.* 57:375–399.

Läuger, P., W. Lesslauer, E. Marti, and J. Richter. 1967. Electrical properties of bimolecular phospholipid membranes. *Biochim. Biophys. Acta.* 135:20–32.

Lesslauer, W., J. Richter, and P. Läuger. 1967. Some electrical properties of bimolecular phosphatidylinositol membranes. *Nature.* 213:1224–1226.

Ludwig, O., V. De Pinto, F. Palmieri, and R. Benz. 1986. Pore formation by the mitochondrial porin of rat brain in lipid bilayer membrane. *Biochim. Biophys. Acta.* 860:268–276.

Mannella, C. A., M. Forte, and M. Colombini. 1992. Toward the molecular structure of the mitochondrial channel, VDAC. *J. Bioenerg. Biomembr.* 24:7–19.

Monticelli, G., E. Gallucci, and S. Micelli. 1990. Experimental data on incorporation of porin molecules in lipid bilayers. *In* Proceedings of the X School on Biophysics of Membrane Transport, Szczyrk, Poland, Vol. 1. 328–343.

Mueller, P., D. O. Rudin, H. Ti Tien, and W. C. Wescott. 1962. Reconstitution of cell membrane structure in *vitro* and its transformation into an excitable system. *Nature.* 194:979–980.

Mueller, P., D. O. Rudin, H. Ti Tien, and W. C. Wescott. 1969. Bimolecular lipid membarnes: technique of formation, study of electrical properties and induction of ionic gating phenomena. *In* Laboratory Technique in Membrane Biophysics. H. Passow and R. Stampfli, editors. Springer, Berlin. 141–145.

Nakae, T. 1976. Identification of the outer membrane protein of *Escherichia coli* that produces transmembrane channels in reconstituted vesicle membranes. *Biochem. Biophys. Res. Commun.* 71:877–889.

Nikaido, H., and M. Vaara. 1985. Molecular basis of bacterial outer membrane permeability. *Microbiol. Rev.* 49:1–32.

Ohki, S. 1969. The electrical capacitance of phospholipid membranes. *Biophys. J.* 9:1195–1205.

Peng, S., E. Blachly-Dyson, M. Colombini, and M. Forte. 1992. Determination of the number of polypeptide subunits in a functional VDAC channel from *Saccharomyces cerevisiae. J. Bioeng. Biomembr.* 24:27–31.

Pfaller, R., H. Freitag, M. A. Harmey, R. Benz, and W. Neupert. 1985. A water soluble form of porin from the mitochondrial outer membrane of *Neurospora crassa. J. Biol. Chem.* 260:8188–8193.

Rosen, D., and A. M. Sutton. 1968. The effect of direct current potential bias on the electrical properties of bimolecular lipid membranes. *Biochim. Biophys. Acta.* 163:226–233.

Rosenbusch, J. P. 1974. Characterization of the major envelope protein from *Escherichia coli. J. Biol. Chem.* 249:8019–8029.

Sachmann, E. 1984. Physical basis of trigger processes and membrane structure. *In* Biological Membranes, Vol. 5. D. Chapman, editor. Academic Press, New York. 105–143.

Sekimuzu, K. 1994. Interactions between DNA replication related proteins and phospholipid vesicles in vitro. *Chem. Phys. Lipids.* 73:223–230.

Ti Tien, H., S. Carbone, and E. A. Dawidowicz. 1966. Procedure for preparation of oxidized cholesterol membrane solution. *Nature.* 212:718–719.

Ti Tien, H., and A. L. Diana. 1968. Bimolecular lipid membranes: a review and a summary of some recent studies. *Chem. Phys. Lipids.* 2:55–101.

Zizi, M., L. Thomas, E. Blachly-Dyson, M. Forte, and M. Colombini. 1995. Oriented channel insertion reveals the motion of a transmembrane beta strand during voltage gating of VDAC. *J. Membr. Biol.* 144: 121–129.